

RESEARCH ARTICLE

MicroRNA-210-mediated mtROS confer hypoxia-induced suppression of STOCs in ovine uterine arteries

Xiang-Qun Hu  | Rui Song | Chiranjib Dasgupta | Monica Romero |
Rucha Juarez | Jenna Hanson | Arlin B. Blood | Sean M. Wilson | Lubo Zhang

Lawrence D. Longo MD Center for Perinatal Biology, Department of Basic Sciences, Loma Linda University School of Medicine, Loma Linda, California, USA

Correspondence

Lubo Zhang, Lawrence D. Longo MD Center for Perinatal Biology, Department of Basic Sciences, Loma Linda University School of Medicine, Loma Linda, CA 92350, USA.
Email: lzhang@llu.edu

Funding information

This work was supported by National Institutes of Health Grants HD083132 (L. Z.), HL128209 (L. Z.), HL137649 (L. Z.), and HL149608 (L. Z.).

Background and Purpose: Hypoxia during pregnancy is associated with increased uterine vascular resistance and elevated blood pressure both in women and female sheep. A previous study demonstrated a causal role of microRNA-210 (miR-210) in gestational hypoxia-induced suppression of Ca^{2+} sparks/spontaneous transient outward currents (STOCs) in ovine uterine arteries, but the underlying mechanisms remain undetermined. We tested the hypothesis that miR-210 perturbs mitochondrial metabolism and increases mitochondrial reactive oxygen species (mtROS) that confer hypoxia-induced suppression of STOCs in uterine arteries.

Experimental Approach: Resistance-sized uterine arteries were isolated from near-term pregnant sheep and were treated *ex vivo* in normoxia and hypoxia (10.5% O_2) for 48 h.

Key Results: Hypoxia increased mtROS and suppressed mitochondrial respiration in uterine arteries, which were also produced by miR-210 mimic to normoxic arteries and blocked by antagonist miR-210-LNA in hypoxic arteries. Hypoxia or miR-210 mimic inhibited Ca^{2+} sparks/STOCs and increased uterine arterial myogenic tone, which were inhibited by the mitochondria-targeted antioxidant MitoQ. Hypoxia and miR-210 down-regulated iron-sulfur cluster scaffold protein (ISCU) in uterine arteries and knockdown of ISCU via siRNAs suppressed mitochondrial respiration, increased mtROS, and inhibited STOCs. In addition, blockade of mitochondrial electron transport chain with antimycin and rotenone inhibited large-conductance Ca^{2+} -activated K^+ channels, decreased STOCs and increased uterine arterial myogenic tone.

Conclusion and Implications: This study demonstrates a novel mechanistic role for the miR-210-ISCU-mtROS axis in inhibiting Ca^{2+} sparks/STOCs in the maladaptation of uterine arteries and provides new insights into the understanding of mitochondrial perturbations in the pathogenesis of pregnancy complications resulted from hypoxia.

Abbreviations: ISCU, iron-sulfur cluster scaffold protein; miR-210, microRNA-210; MitoQ, mitoquinone mesylate; mtROS, mitochondrial reactive oxygen species; OCR, oxygen consumption rate; STOCs, spontaneous transient outward currents.

Xiang-Qun Hu and Rui Song contributed equally.

This is an open access article under the terms of the [Creative Commons Attribution-NonCommercial-NoDerivs](https://creativecommons.org/licenses/by-nc-nd/4.0/) License, which permits use and distribution in any medium, provided the original work is properly cited, the use is non-commercial and no modifications or adaptations are made.

© 2022 The Authors. *British Journal of Pharmacology* published by John Wiley & Sons Ltd on behalf of British Pharmacological Society.

KEYWORDS

Ca²⁺ sparks, hypoxia, mitochondria, pre-eclampsia, pregnancy, reactive oxygen species, STOCs

1 | INTRODUCTION

Hypoxia during pregnancy is an important contributor to the pathogenesis of maternal hypertension and intrauterine growth restriction. Human and animal studies have revealed a causative role of gestational hypoxia in increased uterine vascular resistance and placental hypoxia in pre-eclampsia (Ducsay et al., 2018). Previous studies showed that pregnant sheep are similar to pregnant women in that they both have an increase in uterine vascular resistance and an elevation in maternal systemic blood pressure in response to high altitude hypoxia (Hu et al., 2017; Zamudio et al., 2007). Our recent studies revealed repression of spontaneous transient outward currents (STOCs) to be characteristic of uterine vascular maladaptation to gestational hypoxia and provided evidence of a causal role of microRNA-210 (miR-210) in hypoxia-mediated impairment of Ca²⁺ sparks/STOCs coupling in uterine arteries during gestation in an animal model of pregnant ewes acclimatized to high-altitude hypoxia (Hu et al., 2021, 2019, 2020). Yet, the underlying mechanisms of miR-210-mediated inhibition of Ca²⁺ sparks/STOCs in uterine arteries remain elusive.

The mitochondrion is a major target of miR-210 in the cellular hypoxic response and perturbations of mitochondrial function lead to excessive generation of reactive oxygen species (ROS) and contribute to the pathogenesis of pre-eclampsia (Colleoni et al., 2013; Hu & Zhang, 2021a; Muralimanoharan et al., 2012; Vaka et al., 2019). Among other targets, miR-210 down-regulates a highly conserved protein in mitochondria, the iron-sulfur cluster scaffold protein (ISCU). Down-regulation of ISCU inhibits mitochondrial complex I and III activity and disrupts mitochondrial electron transport. This leads to a switch of energy metabolism from oxidative phosphorylation to glycolysis and an increase in mitochondrial ROS (mtROS) flux (Chan et al., 2009; Chouchani et al., 2014; Colleoni et al., 2013; Favaro et al., 2010; Muralimanoharan et al., 2012; White et al., 2015). However, the mechanisms by which miR-210-mediated mitochondrial perturbations result in suppression of STOCs in uterine arterial maladaptation to gestational hypoxia remain undetermined and are likely to be context and tissue dependent. In the present study, we demonstrate a novel mechanistic link of miR-210-mediated mitochondrial perturbations and mtROS production in hypoxia-induced repression of Ca²⁺ sparks/STOCs coupling in near-term pregnant sheep uterine arteries. We also provide new insights into the understanding of fundamental mechanisms of mitochondrial dysfunction and vascular maladaptation caused by gestational hypoxia and the subsequent maternal complications during pregnancy.

What is already known

- Gestational hypoxia and increased miR-210 inhibit Ca²⁺ sparks and STOCs in uterine arteries.

What does this study add

- MiR-210 mediates hypoxia-induced mitochondrial perturbations and mtROS production in near-term sheep uterine arteries.
- Increased mtROS underlies hypoxia/miR-210-induced suppression of STOCs and increase in myogenic tone in uterine arteries.

What is the clinical significance

- mtROS has key role in uterine vascular homeostasis and in gestational hypoxia pathogenesis complications.
- The present preclinical evidence indicates a therapeutic potential of MitoQ in pre-eclampsia.

2 | METHODS

2.1 | Animal procedures and tissue preparation

All procedures and protocols were approved by the Institutional Animal Care and Use Committee of Loma Linda University and followed the guidelines by the National Institutes of Health Guide for the Care and Use of Laboratory Animals. Time-dated, near-term (~142–145 days of gestation) pregnant sheep (*Ovis aries*) were obtained from Nebeker Ranch (Lancaster, CA, USA). The animals aged 1 year or older with a body weight ranging from 60 to 75 kg. Upon arrival at the LLU animal care facility, the animals were individually caged. Chow Lab Diet Rumi-lab Maintenance 5510 and Southwest Farms Hay replacer (supplied by NEWCO, Rancho Cucamonga, CA, USA), Alfalfa hay (supplied by All Seasons Hay Feed & Ranch Supply, Calimesa, CA, USA), and water were made available ad libitum. Female near-term pregnant sheep were anaesthetized with intravenous injection of propofol (2 mg·kg⁻¹) followed by intubation and anaesthesia was maintained on 1.5–3.0% isoflurane balanced in O₂ throughout the surgery. An incision was made in

the abdomen and the uterus was exposed. Resistance-sized uterine arteries (~150–200 μm in diameter) were isolated without stretching and used in the experiments. After tissue collection, animals were killed via intravenous injection of 15-ml Euthazol[®] (pentobarbital sodium and phenytoin sodium), according to American Veterinary Medical Association guidelines. Animal studies are reported in compliance with the ARRIVE guidelines (Percie du Sert et al., 2020) and with the recommendations made by the *British Journal of Pharmacology* (Lilley et al., 2020).

2.2 | Seahorse assay

Mitochondrial oxygen consumption rate (OCR) was measured in uterine arterial smooth muscle cells using Seahorse XFe24 Analyser (Agilent, Santa Clara, CA) following the manufacturer's protocol. Smooth muscle cells were enzymatically dissociated from uterine arteries, as previously described (Hu et al., 2019). Isolated cells were placed into primary culture in Dulbecco's modified Eagle's medium (DMEM) at 37°C in humidified atmosphere of 5% CO₂ and 95% air, and passages 2–3 were used in the study. Following basal OCR readings, OCR was measured by sequentially treating cells with oligomycin (1.5 μM), carbonyl cyanide-4 (trifluoromethoxy) phenylhydrazone (FCCP, 2 $\mu\text{mol}\cdot\text{L}^{-1}$) and rotenone/antimycin A (0.5 μM) using Cell Mito Stress Test Kit (Agilent). ATP-linked OCR was determined by the difference in OCR before and after the application of the ATP synthase inhibitor oligomycin. The subsequent application of the mitochondrial uncoupler FCCP provided the reading of maximal OCR. In addition, OCR was measured after inhibition of complexes I and III with rotenone and antimycin A to assess nonmitochondrial respiration. Proton leak-linked OCR was determined from the difference between OCR measured following oligomycin and OCR measured after addition of antimycin and rotenone. The results were normalized to total cellular protein concentrations.

2.3 | Measurement of mitochondrial ROS

Mitochondrial ROS (mtROS) were measured in cultured primary uterine arterial smooth muscle cells (passages 2–3) using Mitochondrial ROS Detection Assay Kit (Cayman Chemical Company, Ann Arbor, MI) according to the manufacturer's protocol. The chemiluminescence was detected using a Spark 20M multimode microplate reader (Tecan Group Ltd., Männedorf, Switzerland) and the signal was normalized to total cellular protein concentrations.

2.4 | Measurement of Ca²⁺ sparks

Ca²⁺ sparks were measured in endothelium-denuded uterine arteries loaded with the Ca²⁺ sensitive dye Fluo-4 AM with a Zeiss LSM 710 NLO laser scanning confocal imaging workstation, as previously described (Hu et al., 2019). The arterial segments were pinned to

Sylgard blocks and placed in an open bath imaging chamber mounted on the confocal imaging stage. Cells were illuminated at 488 nm and line scans were imaged at 529 frames s⁻¹ with the emission signal recorded at 493–622 nm. Line scan recordings were analysed for the percent of cells with Ca²⁺ sparks, their frequency, amplitude and other spatiotemporal characteristics via SparkLab 4.3.1 (Hu et al., 2019).

2.5 | Measurement of STOCs

STOCs were recorded in freshly isolated uterine arterial smooth muscle cells in the whole-cell configuration of the perforated patch-clamp technique using an EPC 10 patch-clamp amplifier with Patchmaster software (HEKA, Lambrecht/Pfalz, Germany) at room temperature, as previously described (Hu et al., 2019). Only relaxed and spindle-shaped myocytes were used for recording. Membrane currents were recorded while the cells were held at steady membrane potentials between –50 and 10 mV in 10-mV increments. STOCs were analysed with Mini Analysis program (Synaptosoft, Leonia, NJ) with a threshold for detection setting at 10 pA. The currents were normalized to cell capacitance and expressed as picoampere per picofarad (pA·pF⁻¹).

2.6 | Measurement of pressure-dependent myogenic tone

Pressure-dependent myogenic tone of uterine arteries was measured as described previously (Hu et al., 2011). Briefly, arterial segments were mounted and pressurized in an organ chamber (Living Systems Instruments, Burlington, VT). The intraluminal pressure was controlled by a servo-system to set transmural pressures and arterial diameter was recorded using the SoftEdge Acquisition Subsystem (IonOptix LLC, Milton, MA). After the equilibration period, the intraluminal pressure was increased in a stepwise manner from 10 to 100 mmHg in 10-mmHg increments and each pressure was maintained for 5 min to allow vessel diameter to stabilize before the measurement. Ca²⁺-free physiological saline solution (PSS) contains zero Ca²⁺ and 3-mM EGTA. PSS was allowed to pass through the lumen of the pressurized vessels before detection of myogenic tone and myogenic tone was measured under the static flow. The passive pressure–diameter relationship was conducted in Ca²⁺-free PSS to determine the maximum passive diameter. The following formula was used to calculate the percentage of pressure-dependent tone at each pressure step: % tone = (D1 – D2)/D1 × 100, where D1 is the passive diameter in Ca²⁺-free PSS and D2 is the active diameter with normal PSS in the presence of extracellular Ca²⁺.

2.7 | RNA-induced silencing complex-immunoprecipitation assay

RNA-induced silencing complex-immunoprecipitation assay was performed as previously described (Hu et al., 2021). Cultured primary

uterine arterial smooth muscle cells (passages 2–3) were transfected with $100 \text{ nmol} \cdot \text{L}^{-1}$ miR-210 mimic or the negative scrambled control (Qiagen) by using HiPerfect transfection reagent (Qiagen) according to the manufacturer's instructions. Cells were harvested 24 h after transfection and washed in ice-cold PBS followed by complete lysis buffer (Active Motif) at 4°C for 10 min. RNA-induced silencing complex-immunoprecipitation of the lysate was conducted using the miRNA Target IP Kit (Active Motif) according to the manufacturer's instructions. The RNA was extracted with phenol/chloroform/isoamyl alcohol (25:24:1) once, chloroform once and precipitated and resuspended in RNase-free water. The precipitated RNA was subjected to RT-qPCR using primers specific for the sheep ISCU 3'-UTR. β -actin was used as an internal control. The relative abundance of ISCU transcript pulled down by Ago1/2/3 antibody was calculated by the $2^{-\Delta\Delta\text{CT}}$ method and is presented as the fold induction relative to the control. Primers used were: 5'-GTTTCCTGCAGCTCACTTGC (forward) and 5'-CCCAAACCTGAGACTTCGCT (reverse) for ISCU, and 5'-GCAGTTCATCCATCGGCAAT (forward) and 5'-ACCGTGTGGCG TAGAGTCTCT (reverse) for β -actin.

2.8 | Western immunoblotting

The immuno-related procedures conform the guidelines of the *British Journal of Pharmacology* (Alexander et al., 2018). Protein abundance of ISCU was measured by western immunoblotting, as described previously (Hu et al., 2021). Briefly, tissues were homogenized in a lysis buffer followed by centrifugation at 4°C for 10 min at $10,000g$ and the supernatants were collected. Samples with equal proteins were loaded onto 4–20% polyacrylamide gel (BioRad, Hercules, CA) and were separated by electrophoresis at 180 V for 45 min. Proteins were then transferred onto nitrocellulose membranes. After blocking nonspecific binding sites by dry milk, membranes were incubated with primary antibodies (1:500 dilution) against ISCU1/2 (sc-28860 or sc-373694, Santa Cruz, Dallas, TX). After washing, membranes were incubated with secondary horseradish peroxidase-conjugated antibodies. Proteins were visualized with enhanced chemiluminescence reagents and blots were exposed to Hyperfilm. Results were quantified with the Kodak electrophoresis documentation and analysis system and Kodak ID image analysis software (Kodak, Rochester, NY).

2.9 | Materials

Euthasol[®] (pentobarbital sodium and phenytoin sodium) was obtained from Virbac Corporation, Westlake, TX, USA). The mitochondrial ROS Detection Assay Kit and mitochinone mesylate (MitoQ) were obtained from Cayman Chemical Company (Ann Arbor, MI, USA). Oligomycin, carbonyl cyanide-4(trifluoromethoxy) phenylhydrazone (FCCP) and rotenone/antimycin A were obtained from Sigma-Aldrich (St. Louis, MO, USA). Dulbecco's modified Eagle's medium (DMEM), Fluo-4 AM, phenol, chloroform and

isoamyl alcohol were obtained from Fisher Scientific (Waltham, MA, USA). Antibodies sc-28860 and sc-373694 were obtained from Santa Cruz (Dallas, TX, USA). miR-210 mimic, AllStarsNegative Control siRNA, and HiPerfect transfection reagent were obtained from Qiagen (Germantown, MD, USA).

2.10 | Statistical analysis

Data and statistical analysis comply with the recommendations of the *British Journal of Pharmacology* on experimental design and analysis (Curtis et al., 2018). Studies were designed to generate groups of equal size, using randomisation and blinded analysis. Data were expressed as means \pm SEM obtained from the number of experimental animals. Statistical analyses, undertaken only for studies where each group size was at least $n = 5$, were performed using GraphPad Prism 9 (GraphPad Software, San Diego, CA, USA). Differences were evaluated for statistical significance ($P < 0.05$) by one-way, two-way and repeated measures ANOVA with the post hoc Bonferroni test or t test where appropriate unless specified otherwise. The post hoc test was applied only when F in ANOVA achieved $P < 0.05$. F test was performed to check whether the variances of the individual groups were homogeneous. If not, Mann-Whitney U -test was used.

2.11 | Nomenclature of targets and ligands

Key protein targets and ligands in this article are hyperlinked to corresponding entries in the IUPHAR/BPS Guide to PHARMACOLOGY <http://www.guidetopharmacology.org> and are permanently archived in the Concise Guide to PHARMACOLOGY 2021/22 (Alexander et al., 2021).

3 | RESULTS

3.1 | MiR-210 mediates hypoxia-induced mitochondrial perturbations and mtROS generation

The effect of hypoxia and miR-210 on mitochondrial respiration (oxygen consumption rate, OCR) in primary cultured ovine uterine arterial smooth muscle cells derived from near-term pregnant sheep were determined using Seahorse XFe24 analyser. Culture under hypoxia (10.5% O_2) had no significant effect on gross morphology of the isolated smooth muscle cells (Figure S1). The real-time traces and average data of OCR measurements are shown in Figure 1a,b. The hypoxia (10.5% O_2) treatment for 48 h significantly decreased basal and maximal mitochondrial OCR as compared with the control (21% O_2), which was recovered by inhibition of miR-210 with antagomir miR-210-LNA (Figure 1a,c). In addition, the miR-210 mimic treatment simulated the effect of hypoxia and resulted in a significant decrease in basal and maximal mitochondrial respiration

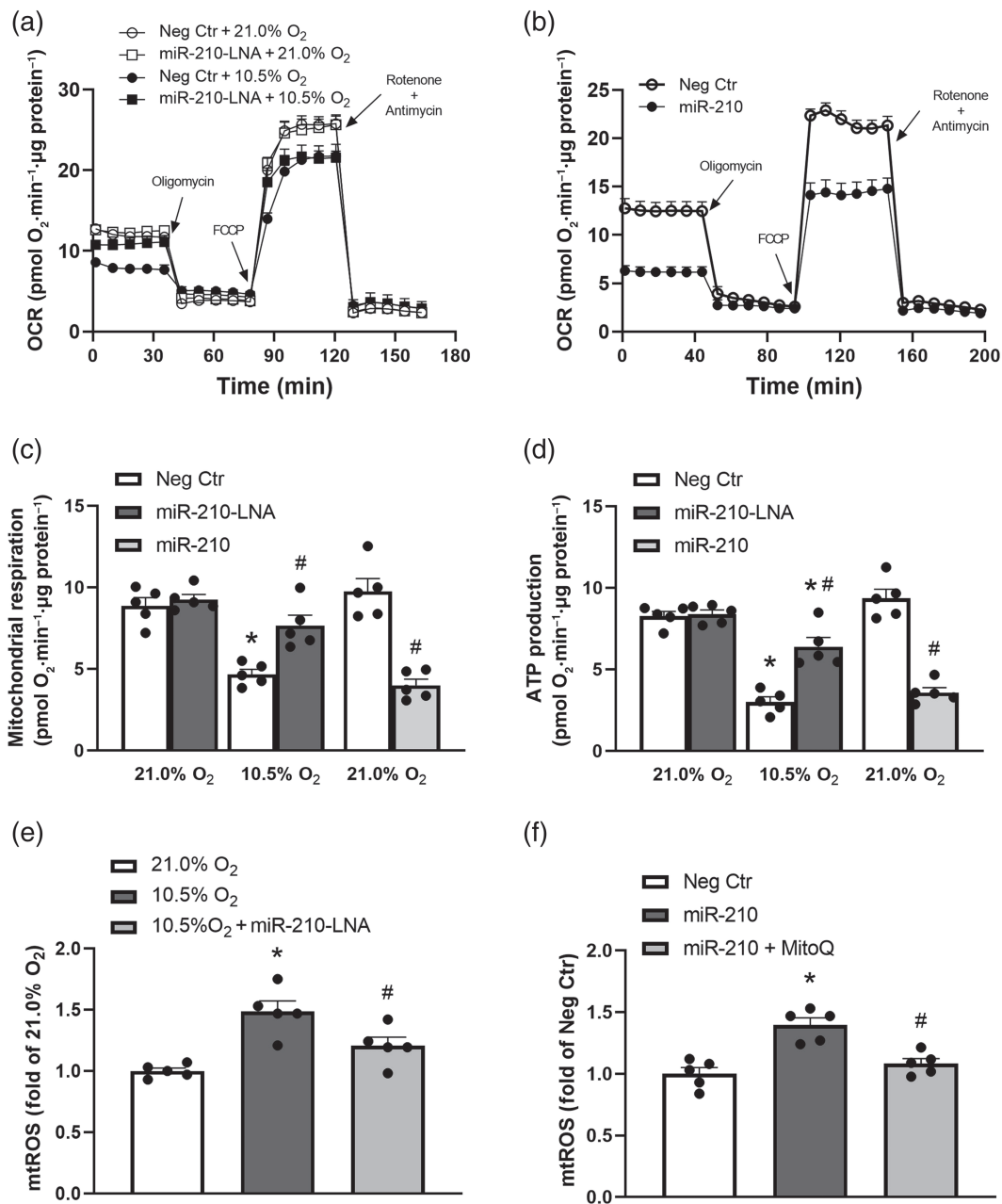


FIGURE 1 Effect of hypoxia and miR-210 on mitochondrial respiration and mitochondrial reactive oxygen species (mtROS) production in uterine arteries. Uterine arteries were isolated from near-term pregnant sheep and mitochondrial oxygen consumption rate (OCR) was determined by Seahorse XFe24 Analyser in cultured primary smooth muscle cells treated under 21.0% and 10.5% O₂ in the presence of miR-210-LNA (100 nM) or negative control (Neg Ctr) for 48 h (a) and under 21.0% O₂ in the presence of miR-210 mimic (100 nM) or negative control (Neg Ctr) for 48 h (b). Effects of miR-210-LNA and miR-210 on mitochondrial respiration (c) and ATP production (d) under 10.5% O₂ and 21.0% O₂, respectively. Data are means ± SEM. *n* = 5 measurements in cells pooled from five animals. **P* < 0.05, versus 21.0% O₂; #*P* < 0.05, versus Neg Ctr. Mitochondria-derived ROS (mtROS) was measured with Mitochondrial ROS Detection Assay Kit in uterine arterial smooth muscle cells treated under 21.0% O₂ and 10.5% O₂ in the absence or presence of miR-210-LNA (100 nM) for 48 h (e) and under 21.0% O₂ in the absence or presence of miR-210 mimic (100 nM) or miR-210 plus mitoquinone mesylate (MitoQ; 1 µM) for 48 h (f). Data are means ± SEM. *n* = 5 measurements in cells pooled from five animals. **P* < 0.05, 10.5% O₂ versus 21.0% O₂; #*P* < 0.05, 10.5% O₂ + miR-210-LNA versus 10.5% O₂. (e) **P* < 0.05, miR-210 versus Neg Ctr; #*P* < 0.05 miR-210 + MitoQ versus miR-210 (f). FCCP: carbonyl cyanide-4 (trifluoromethoxy) phenylhydrazone

(Figure 1b,c). In accordance, ATP-linked OCR was reduced by hypoxia and miR-210-LNA partially blocked the hypoxic effect (Figure 1a,d). In a way similar to hypoxia, miR-210 mimic

substantially decreased ATP-linked OCR (Figure 1b,d). Mitochondrial respiration, non-mitochondrial respiration, spare capacity and proton leak-linked OCR were not significantly altered by hypoxia,

miR-210-LNA and miR-210 mimic (Table S1). As mitochondria are the main source of ROS, we next examined a mechanistic link of miR-210 in the regulation of mtROS production in response to hypoxia. As shown in Figure 1e, hypoxia significantly increased mtROS production in uterine arterial smooth muscle cells, which was abolished by inhibition of miR-210 with miR-210-LNA. In addition, the approach of gain-of-function showed that miR-210 mimic increased mtROS in cultured uterine arterial smooth muscle cells, which was reversed by the presence of mitochondria-specific antioxidant, MitoQ (Figure 1f). In contrast, MitoQ had no effect on mtROS production in cultured uterine arterial smooth muscle cells under normoxia (Figure S2).

3.2 | mtROS mediate hypoxia-induced suppression of STOCs

Our previous study showed that gestational hypoxia inhibited STOCs in ovine uterine arteries from near-term (~142-145 days of gestation) pregnant sheep (Hu et al., 2020). We reasoned that hypoxia-induced increases in mtROS might contribute to the suppression of STOCs. To this end, near-term pregnant sheep uterine arteries were treated with hypoxia (10.5% O₂) in the absence or presence of MitoQ for 48 h and

STOCs in freshly isolated smooth muscle cells were subsequently measured. Figure 2a illustrates STOCs recorded at 10 mV in myocytes under normoxia (21.0% O₂) and hypoxia (10.5% O₂) in the presence of 1- μ M MitoQ. Consistent with the previous findings (Hu et al., 2020), the hypoxia treatment significantly reduced both STOC frequency and amplitude (Figure 2b,c). Of importance, MitoQ blocked the effect of hypoxia-induced repression of STOCs in uterine arteries (Figure 2b,c). In contrast, MitoQ had no effect on both STOC frequency and amplitude in uterine arteries under 21.0% O₂ (Figure S3A,B).

3.3 | MitoQ blocks the effect of miR-210 on Ca²⁺ sparks/STOCs and myogenic tone

Hypoxia increased miR-210 in ovine uterine arteries from near-term (~142-145 days of gestation) pregnant sheep (Hu et al., 2017), which conferred hypoxia-induced suppression of Ca²⁺ sparks and STOCs, as well as increase in pressure-dependent myogenic tone in uterine arteries (Hu et al., 2021, 2017). We subsequently explored the role of mtROS in miR-210-mediated suppression of Ca²⁺ sparks and STOCs as well as increase in uterine arterial myogenic tone. Consistent with the previous findings, miR-210 significantly decreased both Ca²⁺

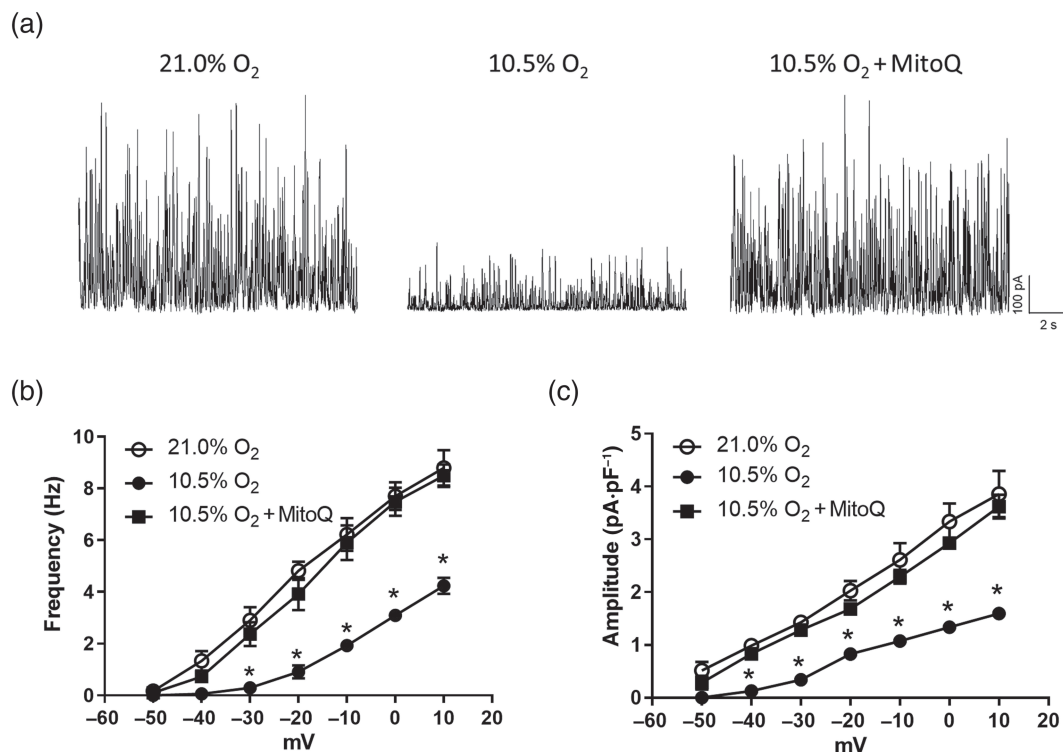


FIGURE 2 Effect of mitoquinone mesylate (MitoQ) on hypoxia-induced suppression of spontaneous transient outward currents (STOCs) in uterine arteries. Uterine arteries were isolated from near-term pregnant sheep and treated under 21.0% O₂ and 10.5% O₂ in the absence or presence of MitoQ (1 μ M) for 48 h. (a) Representative STOC tracings recorded at 10 mV in freshly isolated smooth muscle cells. (b and c) Summary data of STOC frequency (b) and amplitude (c). Data are means \pm SEM. *N* = 5 animals in each group, and all data points from one single animal were pooled to a common data point. **P* < 0.05, 10.5% O₂ versus 21.0% O₂

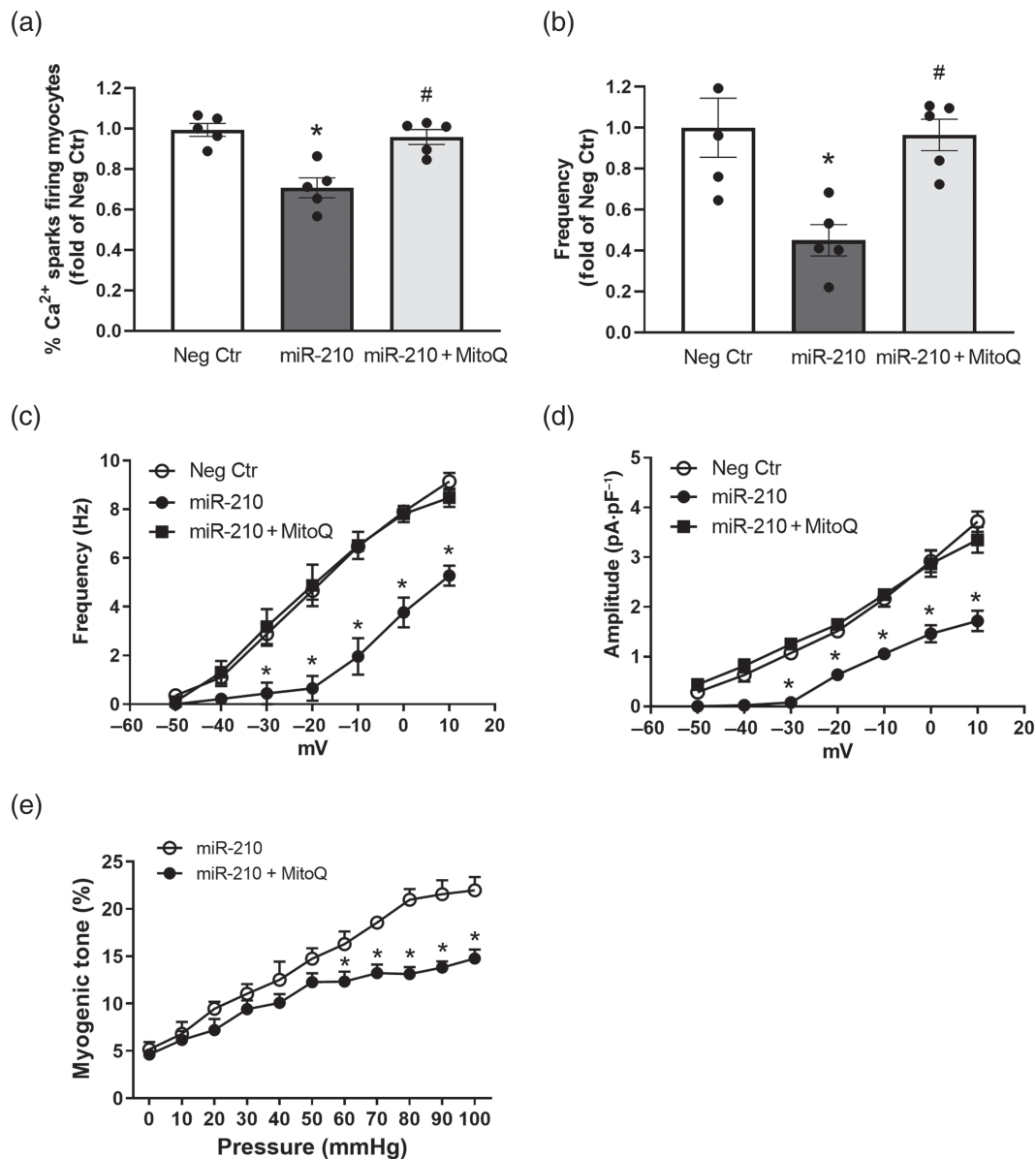


FIGURE 3 Effect of mitoquinone mesylate (MitoQ) on miR-210-induced suppression of Ca^{2+} sparks and spontaneous transient outward currents (STOCs) in uterine arteries. Uterine arteries were isolated from near-term pregnant sheep and treated with miR-210 (100 nM) or negative control (Neg Ctr) under 21.0% O_2 in the absence or presence of MitoQ (1 μM) for 48 h. Percentage of myocytes with Ca^{2+} sparks (a, Neg Ctr: 67.2 ± 5.1) and Ca^{2+} spark frequency (b, Neg Ctr: 0.0085 ± 0.0012 sparks $\mu\text{m}^{-1} \text{s}^{-1}$), STOC frequency (c) and amplitude (d), and pressure-dependent myogenic tone (e) were measured. Data are means \pm SEM. $n = 5$ animals in each group. For Ca^{2+} sparks and STOCs measurements, all data points from one single animal were pooled to a common data point. * $P < 0.05$, miR-210 versus Neg Ctr; # $P < 0.05$, miR-210 + MitoQ versus miR-210

spark-firing myocytes and Ca^{2+} spark frequency in uterine arterial smooth muscle cells (Figure 3a,b). Of importance, MitoQ blocked the effect of miR-210 and recovered Ca^{2+} sparks (Figure 3a,b). Accordingly, miR-210 suppressed both STOC frequency and amplitude, and MitoQ abolished miR-210-mediated inhibition of STOCs (Figure 3c,d). Furthermore, MitoQ significantly decreased miR-210-induced myogenic tone of uterine arteries (Figure 3e). In contrast, MitoQ had no effect on Ca^{2+} sparks (Figure S4) and myogenic tone (Figure S5) in the control groups.

3.4 | Knockdown of iron-sulfur cluster scaffold protein (ISCU) independent of miR-210 in the uterine artery increases mtROS and inhibits STOCs

ISCU is of critical importance in mitochondrial complex I and III activity, and down-regulation of ISCU impairs mitochondrial electron transport and increases mitochondrial ROS flux. As shown in Figure 4a, the hypoxia treatment of near term uterine arteries significantly decreased ISCU protein abundance. ISCU is a conserved target of

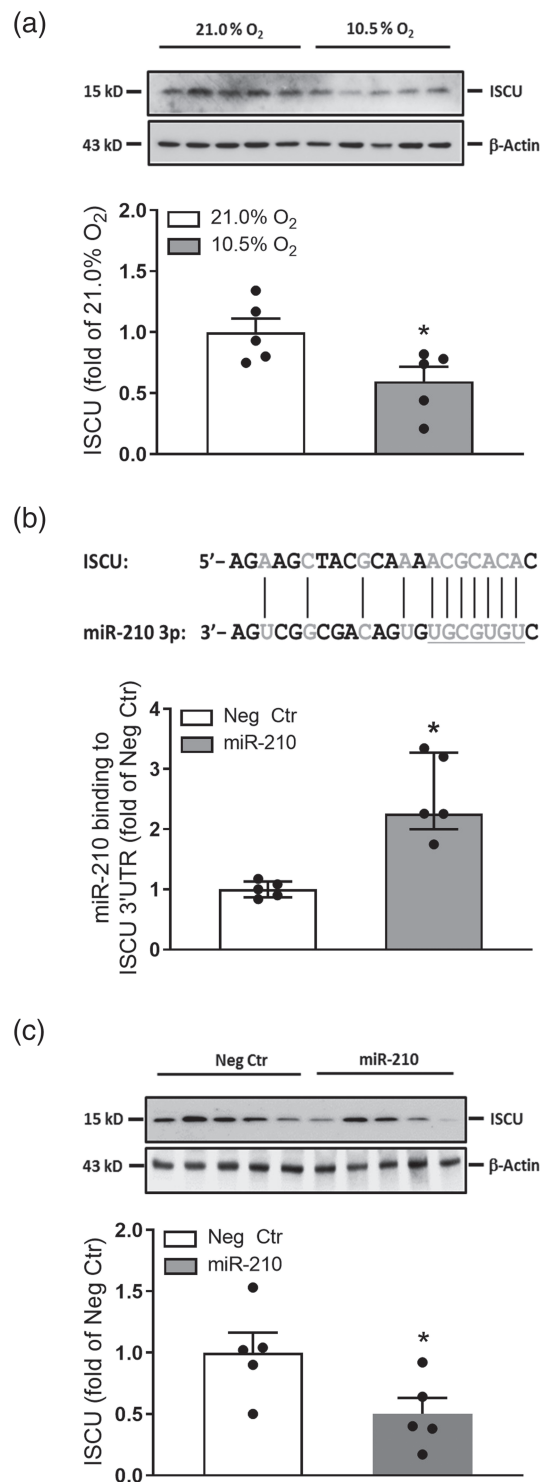


FIGURE 4 Effect of hypoxia and miR-210 on iron–sulfur cluster scaffold protein (ISCU) protein expression in uterine arteries. (a) Uterine arteries were isolated from near-term pregnant sheep and treated under 21.0% O₂ and 10.5% O₂ for 48 h. ISCU protein abundance was determined by western blots using the monoclonal antibody against ISCU1/2 (D-6, sc-373694). Data are means ± SEM of five animals in each group. **P* < 0.05, 10.5% O₂ versus 21.0% O₂. (b) Schematic representation of alignment of miR-210 binding site to ovine ISCU 3'-untranslated region (3' UTR) is shown. RNA-induced silencing complex-immunoprecipitation (RISC-IP) analysis of abundance of ISCU 3' UTR pulled down by Ago1/2/3 antibody in cultured primary uterine arterial smooth muscle cells transfected with miR-210 (100 nM) or negative control (Neg Ctr) for 24 h. *F* test showed that the variances of the individual groups were not homogeneous. The data are presented as medians and interquartile ranges (IQRs) and analysed using Mann–Whitney *U*-test. *n* = 5 measurements in cells pooled from five animals. **P* < 0.05, miR-210 versus Neg Ctr. (c) Uterine arteries were treated with miR-210 (100 nM) or negative control (Neg Ctr) under 21.0% O₂ for 48 h. ISCU protein abundance was determined by western blots using the monoclonal antibody against ISCU1/2 (D-6, sc-373694). Data are means ± SEM of five animals in each group. **P* < 0.05, miR-210 versus Neg Ctr

miR-210 and ovine ISCU transcript 3'-untranslated region contains miR-210 complementary binding sites (Figure 4b). Our previous study demonstrated the binding of miR-210 to the 3'-untranslated region of ISCU (Ma et al., 2019). miRNAs exert their regulatory effects primarily through base-pairing with their target mRNAs in a complex with RISC (RNA-induced silencing complex) and RNA-induced silencing complex-immunoprecipitation assay has been widely used to identify the binding of miRNAs to the 3'-untranslated region of target mRNAs (Ding & Wang, 2011). We thus determined whether ovine ISCU is a genuine target of miR-210. RNA-induced silencing complex-immunoprecipitation assay revealed that ISCU 3'-untranslated region binding to miR-210 was increased by ~2-fold in miR-210-treated uterine arterial smooth muscle cells, compared with negative control-treated cells (Figure 4b). Moreover, the miR-210 treatment significantly decreased ISCU protein abundance in uterine arteries (Figure 4c), indicating that ovine ISCU is a target of miR-210.

To demonstrate a causal role of ISCU in the actions of miR-210 and hypoxia in the regulation of mitochondrial respiration and mtROS production, we assessed the consequences of repressing ISCU with siRNAs in uterine arteries independent of hypoxia or miR-210 manipulation. Compared with control siRNA-treated tissues, uterine arteries that were treated with siRNAs targeting ovine ISCU exhibited a ~50% decrease in ISCU protein abundance (Figure 5a), a consequent decrease in basal mitochondrial OCR and ATP-linked OCR (Figure 5b,c), and an increase in mtROS (Figure 5d). Non-mitochondrial respiration, spare capacity, and proton leak-linked OCR were not significantly altered (Table S1). As a result, ISCU knockdown resulted in a significant decrease in both STOC frequency and amplitude in uterine arteries as compared with the control siRNA treatment (Figure 5e,f). Thus, similar to both hypoxia and miR-210 mimic, independent knockdown of ISCU promotes the phenotype of STOC repression in uterine arteries, thereby confirming the direct importance of mitochondrial energy metabolism in uterine vascular homeostasis in response to hypoxia.

3.5 | Pharmacological inhibition of mitochondrial complexes I and III suppresses STOCs and increases myogenic tone

To substantiate the importance of mitochondrial electron transport and energy metabolism in the regulation of STOCs in uterine arteries from near-term (142-145 days of gestation) pregnant sheep, **large-conductance Ca²⁺-activated K⁺ (BK_{Ca}) channel** (BK_{Ca}, K_{Ca}1.1) activity and STOCs were measured following pharmacologically inhibiting the electron transport chain in mitochondria. The application of complex I inhibitor rotenone (10 μM) or complex III inhibitor antimycin (10 μM) decreased BK_{Ca} channel activity in uterine arterial smooth muscle cells (Figure 6a,b). Accordingly, STOCs were suppressed by both antimycin and rotenone (Figure 6c,d). Moreover, antimycin or rotenone significantly increased pressure-dependent myogenic tone in uterine arteries and the combined use of both produced an additive effect on myogenic tone (Figure 6e).

4 | DISCUSSION

Gestational hypoxia via increasing miR-210 has been shown to suppress Ca²⁺ sparks/ spontaneous transient outward currents (STOCs) coupling in ovine uterine arteries from near-term pregnant sheep, resulting in increased uterine vascular resistance. Emerging evidence suggests that miR-210 is a major regulator of mitochondrial function in the cellular hypoxic response. In the present study, we investigated a mechanistic link of the miR-210-ISCU-mtROS axis to uterine vascular malfunction in response to hypoxia. Our major findings are: (1) hypoxia via miR-210 stimulates mtROS production and impairs mitochondrial respiration, resulting in suppression of Ca²⁺ sparks/STOCs and an increase in uterine arterial myogenic tone, (2) hypoxia down-regulates iron-sulfur cluster scaffold protein (ISCU) and ovine ISCU is a direct target of miR-210, (3) knockdown of ISCU independent of hypoxia and miR-210 in the uterine artery decreases mitochondrial energy metabolism, increases mtROS and inhibits STOCs and (4), pharmacological inhibition of mitochondrial electron transport chain promotes both suppression of STOCs and the increase in uterine arterial myogenic tone.

The mitochondrion is a major target of cellular hypoxia and perturbations of mitochondrial energy metabolism and ROS production play a central role in the cellular stress response (Lee et al., 2020). We demonstrate that hypoxia reduces mitochondrial energy metabolism and increases mtROS in uterine arteries. This is consistent with our previous findings that gestational hypoxia promoted oxidative stress in uterine arteries (Hu et al., 2016; Xiao et al., 2013), suggesting that mitochondrial perturbations and mtROS production contribute to hypoxia-induced oxidative stress. Similarly, chronic hypoxia inhibited oxidative phosphorylation and induced mtROS generation in rodent placentas, in human placental explants and in cultured human trophoblasts (Aljunaidy et al., 2018; Matheson et al., 2016; Vangrieken, Al-Nasiry, Bast, Leermakers, Tulen, Janssen, et al., 2021a). Likewise, chronic hypoxia also increased mtROS in cultured rat pulmonary arterial smooth muscle cells (Waypa et al., 2010). Uteroplacental tissues manifest a hypoxic phenotype and hypoxia is believed to be a primary trigger of pre-eclampsia (Ducsay et al., 2018; Soleymanlou et al., 2005; Tong & Giussani, 2019). As expected, pre-eclamptic placentas displayed both impaired mitochondrial metabolism and elevated mtROS (Hu & Zhang, 2021a; Marin et al., 2020; Vangrieken, Al-Nasiry, Bast, Leermakers, Tulen, Schiffers, et al., 2021b; Wang & Walsh, 1998). Similar findings were also observed in placentas from a rat model of pre-eclampsia induced by reduced uterine perfusion pressure (Vaka et al., 2018).

miR-210 is a target of HIF1 α , and both miR-210 and HIF1 α are master regulators of the cellular hypoxic response (Chan et al., 2012; Huang et al., 2010; Loscalzo, 2010). Mature miR-210 of 22 nt is highly homologous across species and is identical among the human, sheep and rodent. Of importance, an increase in miR-210 appears to be a common mechanism in pre-eclampsia and gestational hypoxia. Elevated placental expression of miR-210 and circulating miR-210 levels have been demonstrated in both pre-eclampsia and pregnancy at high altitude in pregnant women (Colleoni et al., 2013; Muralimanoharan

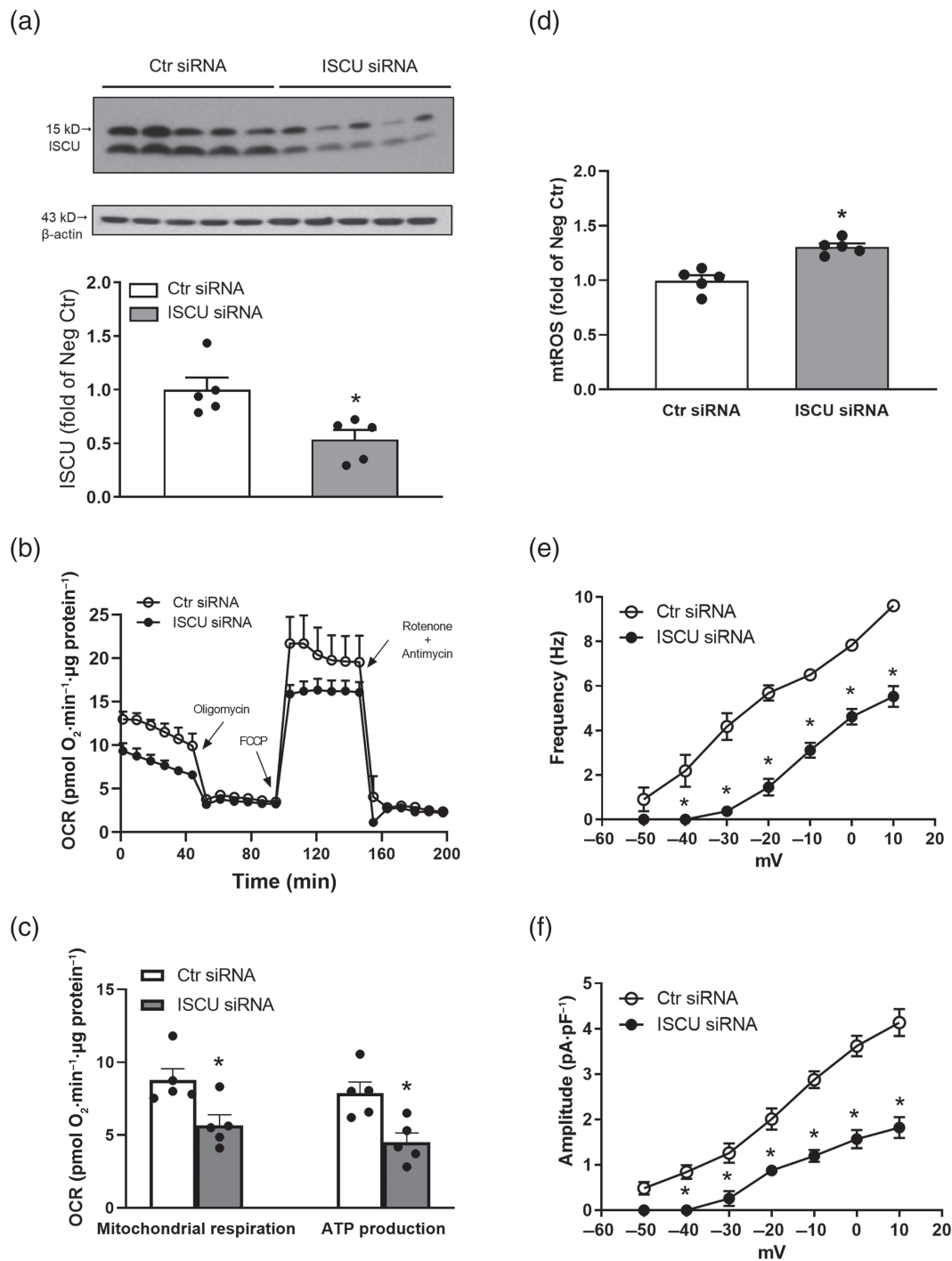


FIGURE 5 Effect of iron-sulfur cluster scaffold protein (ISCU) knockdown on mitochondrial dysfunction and spontaneous transient outward currents (STOCs) suppression in uterine arteries. Cultured uterine arteries from near-term (142-145 days of gestation) pregnant sheep were treated with ovine ISCU siRNA (100 nM) or scramble control (Ctr siRNA) for 48 h. (a) ISCU protein abundance was determined by western blots using the polyclonal antibody against ISCU1/2 (FL-142, sc-28860). Data are means \pm SEM of five animals in each group. * $P < 0.05$, ISCU siRNA versus Ctr siRNA. (b, c) Mitochondrial oxygen consumption rate (OCR) was determined with Seahorse XFe24 Analyser and (d) mitochondria-derived ROS (mtROS) was measured with Mitochondrial ROS Detection Assay Kit in cultured primary uterine arterial smooth muscle cells. Data are means \pm SEM. $n = 5$ measurements in cells pooled from five animals. * $P < 0.05$, ISCU siRNA versus Ctr siRNA. (e, f) STOC frequency and amplitude. Data are means \pm SEM. $N = 5$ animals in each group, and all data points from one single animal were pooled to a common data point. * $P < 0.05$, ISCU siRNA versus Ctr siRNA

et al., 2012; Wu et al., 2012; Zhang et al., 2012). We have demonstrated significant increases in HIF1 α and miR-210 in uterine arteries and plasma miR-210 levels in pregnant sheep acclimatized to high

altitude hypoxia (Hu et al., 2021, 2017). The present study provides evidence of a mechanistic link of miR-210 in hypoxia-mediated perturbations of mitochondrial energy metabolism and mtROS

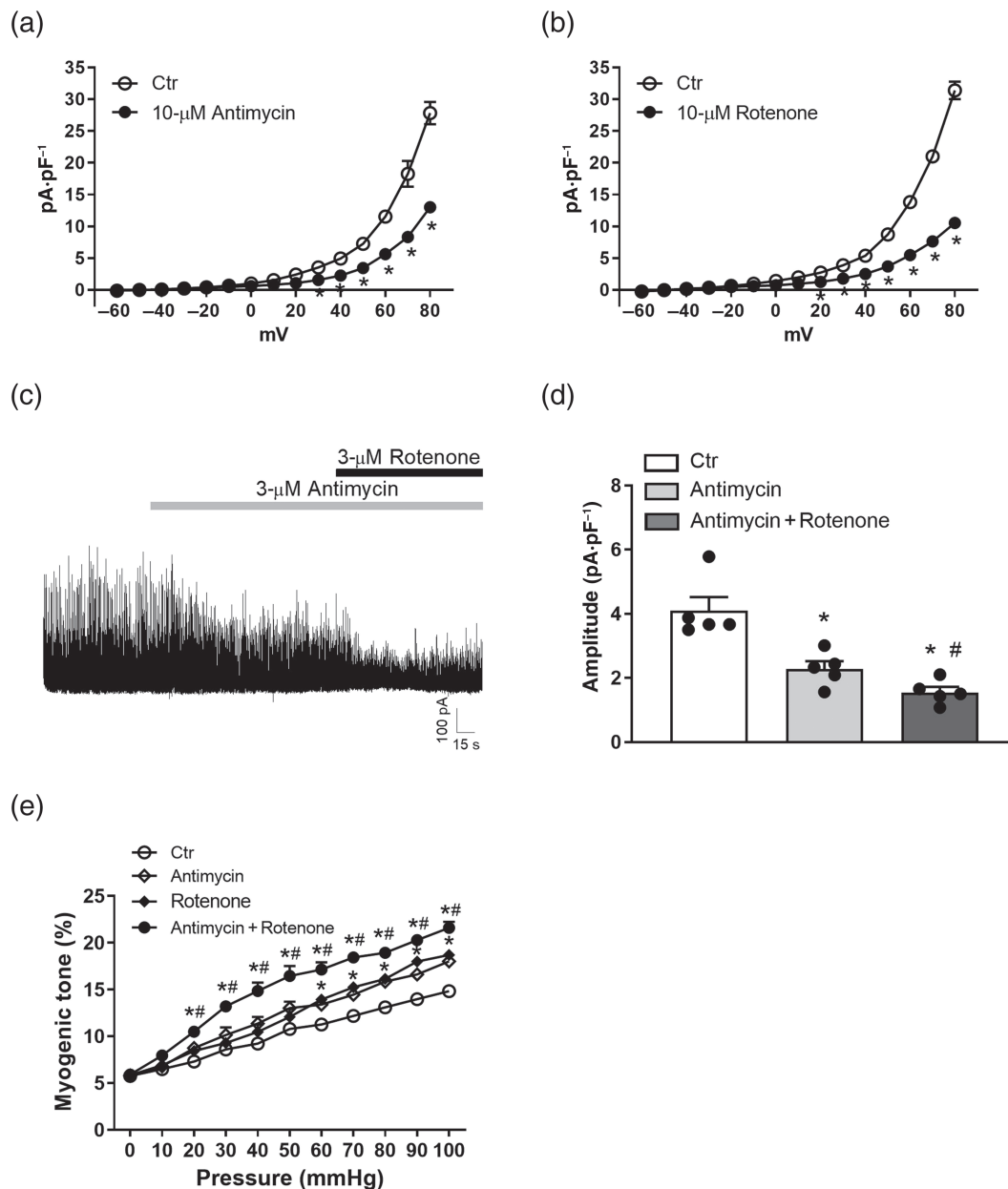


FIGURE 6 Effect of rotenone and antimycin on spontaneous transient outward currents (STOCs), and myogenic tone in freshly isolated uterine arteries from near-term (142–145 days of gestation) pregnant sheep. (a and b) Freshly isolated uterine arterial smooth muscle cells were treated with antimycin (10 μM) or rotenone (10 μM). BK_{Ca} channel currents were measured by voltage steps from –60 mV to +80 mV by stepwise 10-mV depolarizing pulses (350-ms duration, 10-s intervals). Data are means ± SEM. *n* = 5 animals in each group and all data points from one single animal were pooled to a common data point. **P* < 0.05, treatment versus Ctr. (c, d) Freshly isolated uterine arterial smooth muscle cells were treated with a consecutive application of antimycin (3 μM) and rotenone (3 μM), and STOCs were recorded. Data are means ± SEM. *n* = 5 animals in each group and all data points from one single animal were pooled to a common data point. **P* < 0.05, antimycin versus Ctr; #*P* < 0.05, antimycin + rotenone versus antimycin. (e) Uterine arterial myogenic tone in the absence or presence of antimycin (3 μM), rotenone (3 μM) and antimycin + rotenone. Data are means ± SEM of five animals in each group. **P* < 0.05, treatment versus Ctr; #*P* < 0.05, antimycin + rotenone versus antimycin or rotenone alone

production. This concept is supported by following findings with the approaches of loss-of-function and gain-of-function experiments: - (1) inhibition of endogenous miR-210 with miR-210-LNA alleviated hypoxia-induced both suppression of mitochondrial energy metabolism and increase in mtROS, and (2) exogenous miR-210 expression promoted a hypoxic phenotype (i.e. increased mtROS and reduced

mitochondrial energy metabolism), which was blocked by the mitochondria-targeted antioxidant MitoQ. The actions of miR-210 are not limited to uterine arteries. Similarly, miR-210 played a key role in disrupting mitochondrial respiration in extravillous trophoblasts and pre-eclamptic and high-altitude placentas (Anton et al., 2019; Colleoni et al., 2013; Muralimanoharan et al., 2012). Interestingly, pulmonary

and uteroplacental circulation share many similarities in response to hypoxia (Hu & Zhang, 2021b). Not surprisingly, hypoxia via miR-210 also increased mtROS in primary human pulmonary arterial endothelial cells, leading to the development of pulmonary hypertension (Chan et al., 2009; White et al., 2015). In addition, hypoxia-induced increase in miR-210 caused mitochondrial dysfunction and promoted mtROS production in cancer cell lines and neurons (Favaro et al., 2010; Ma et al., 2019). However, elevated miR-210 was also shown to suppress mtROS in other cells including neonatal rat cardiomyocytes and C2C12 skeletal muscle cells (Cicchillitti et al., 2012; Mutharasan et al., 2011), suggesting that the effect of miR-210 is context- and tissue-dependent.

miR-210 exerts its actions via targeting an array of genes (Bavelloni et al., 2017). Among them, *ISCU* is a mitochondria-related gene encoding the scaffold protein ISCU. Our previous (Hu et al., 2017) and present studies revealed that the expression of miR-210 and *ISCU* in uterine arteries exhibited a reciprocal pattern in response to hypoxia, that is, increased levels of miR-210 and reduced abundance of *ISCU*. In alignment with findings in other cells and/or tissues (Anton et al., 2019; Chan et al., 2009; Colleoni et al., 2013; Favaro et al., 2010; Ma et al., 2019; Muralimanoharan et al., 2012; White et al., 2015), we found that *ISCU* is a direct target of miR-210 in ovine uterine arteries, and miR-210 evidently mediated hypoxia-induced down-regulation of *ISCU*. In the mitochondrion, Fe-S clusters are integrated into complexes I-III where they function as protein cofactors involved in facilitating electron transport (Maio et al., 2017). The down-regulation of *ISCU* impairs the Fe-S cluster assembly and inhibits electron transport across the electron transport chain, resulting in reduced mitochondrial respiration/ATP production. In addition, the malfunction of Fe-S clusters leads to increased accumulation of electrons and promotes mtROS generation. These concepts are demonstrated by findings from knockdown of *ISCU* independent of hypoxia and miR-210 in uterine arteries. In a way similar to hypoxia exposure and miR-210 transfection, *ISCU* siRNAs suppressed mitochondrial respiration/ATP production and increased mtROS in uterine arterial smooth muscle cells. Likewise, miR-210-induced *ISCU* down-regulation accounted for impaired mitochondrial respiration and elevated mtROS in pre-eclamptic and high-altitude placentas and hypoxia-exposed trophoblasts (Anton et al., 2019; Colleoni et al., 2013; Muralimanoharan et al., 2012). Together, these findings establish a critical role of the miR-210-*ISCU* axis in mitochondrial perturbations and mtROS generation in pregnancy complications associated with hypoxia.

Of importance, the present study provides novel evidence of a mechanistic link of miR-210-*ISCU*-mtROS axis in inhibiting Ca^{2+} sparks/STOCs in the maladaptation of uterine arteries to hypoxia. STOCs at physiological membrane potentials of vascular smooth muscle cells fundamentally regulate vascular myogenic tone and blood flow in an organ, as well as arterial blood pressure. We demonstrated in sheep that pregnancy significantly increased STOCs in uterine arteries (Hu et al., 2019). Of importance, our recent study revealed that high-altitude hypoxia suppressed this pregnancy-induced up-regulation of STOCs (Hu et al., 2020) and provided

evidence of a causal role of miR-210 in hypoxia-mediated impairment of Ca^{2+} spark/STOC coupling in uterine arteries (Hu et al., 2021). Dysregulation of mtROS leads to oxidative stress and has been associated with vascular dysfunction (Freed & Gutterman, 2013). For instance, mtROS contributed to chronic hypoxia-induced increase in basal pulmonary arterial tone in neonatal rats (Sheak et al., 2020). In the present study, we showed that hypoxia increased mtROS through miR-210-mediated down-regulation of *ISCU* in uterine arteries. The elevated mtROS conferred hypoxia- and/or miR-210-mediated inhibition of Ca^{2+} sparks and STOCs in uterine arteries as MitoQ alleviated the inhibition. Ca^{2+} sparks are mediated by **ryanodine receptors**, whereas STOCs are conducted by BK_{Ca} channels. Both ryanodine receptors and BK_{Ca} channels contain various cysteine residues and are subject to redox modulation (Nikolaienko et al., 2018; Tang et al., 2001). Prolonged exposure to H_2O_2 promoted **RyR2** inhibition (Zissimopoulos & Lai, 2006). In isolated rat cardiac myocytes, photoactivated mtROS elicited a transient increase in Ca^{2+} sparks followed by a gradual suppression of Ca^{2+} sparks (Yan et al., 2008). We have shown that RyR2 is the major subtype of ryanodine receptors to generate Ca^{2+} sparks in uterine arteries (Song et al., 2021). Furthermore, we demonstrate in the present study that mtROS accounted for miR-210-induced suppression of both Ca^{2+} spark-firing myocytes and Ca^{2+} spark frequency in uterine arteries. H_2O_2 also suppressed BK_{Ca} channel activity via oxidation of cysteine 911 of the α subunit (Tang et al., 2004). Indeed, STOCs in uterine arteries were inhibited by mtROS induced by hypoxia/miR-210. Further evidence of the link between mitochondrial perturbations and mtROS in regulating STOCs is provided by the findings of pharmacological inhibition of mitochondrial complex I and III. Rotenone and antimycin are inhibitors of complexes I and III in the ETC, respectively, and stimulate ROS generation in mitochondria (Chaplin et al., 2015; Fato et al., 2009). In a way, similar to hypoxia and miR-210, we found that pharmacological inhibition of complexes I and III by rotenone and antimycin suppressed STOCs and increased pressure-dependent myogenic tone in uterine arteries. Similar findings were obtained in rat cerebral arteries, showing that rotenone suppressed both Ca^{2+} sparks and STOCs (Cheranov & Jaggar, 2004). Thus, similar to both hypoxia and miR-210 mimic, independent knockdown of *ISCU* or inhibition of mitochondrial electron transport chain promoted the phenotypic repression of STOCs and increase in myogenic tone in uterine arteries. Thereby showing the direct importance of mitochondrial metabolism and mtROS in uterine vascular homeostasis in response to hypoxia.

5 | CONCLUSION

The present study reveals a novel mechanistic link of miR-210-*ISCU*-mtROS axis in inhibiting Ca^{2+} sparks/STOCs in the maladaptation of uterine arteries. It also provides new insights into the understanding of fundamental mechanisms of mitochondrial perturbations and mtROS in the pathogenesis of pregnancy complications associated with gestational hypoxia. The findings also present preclinical

evidence of a promising therapeutic approach of MitoQ in pre-eclampsia associated with hypoxia. MitoQ has been shown to prevent oxidative stress and to improve both mitochondrial dysfunction/stress in placentas and foetal growth restriction induced by either chronic hypoxia (Aljunaidy et al., 2018; Botting et al., 2020; Ganguly et al., 2021; Nuzzo et al., 2018; Phillips et al., 2017) or by reduced uterine perfusion pressure (Vaka et al., 2018). Of critical importance, MitoQ has been in multiple clinical trials including that of pulmonary artery hypertension and hypertension where it has been found to be well-tolerated in human studies (Rossman et al., 2018; Zinovkin & Zamyatnin, 2019). Although it is outside the scope of this study and it warrants a separate study, *in vivo* evidence that knockdown of miR-210 could alleviate pregnancy complications remains intriguing for future investigation.

ACKNOWLEDGEMENTS

A portion of this research used the Loma Linda University School of Medicine Advanced Imaging and Microscopy Core, a facility supported in part by the National Science Foundation through the Major Research Instrumentation program of the Division of Biological Infrastructure Grant No. 0923559 and the Loma Linda University School of Medicine.

AUTHOR CONTRIBUTIONS

X-Q.H., R.S. and L.Z. conceived the study. X-Q.H., R.S., C.D., M.R., R.J., J.H. and S.M. acquired and/or analysed data. L.Z. supervised the project. X-Q.H., R.S., A.B.B., S.M. and L.Z. drafted and revised the manuscript. All authors reviewed the final version and approved manuscript submission.

CONFLICT OF INTEREST

None declared.

DECLARATION OF TRANSPARENCY AND SCIENTIFIC RIGOUR

This Declaration acknowledges that this paper adheres to the principles for transparent reporting and scientific rigour of preclinical research as stated in the *BJP* guidelines for [Design and Analysis](#), [Immunoblotting and Immunochemistry](#) and [Animal Experimentation](#), and as recommended by funding agencies, publishers, and other organizations engaged with supporting research.

DATA AVAILABILITY STATEMENT

Data are available on request from the authors.

ORCID

Xiang-Qun Hu  <https://orcid.org/0000-0003-1626-9541>

REFERENCES

Alexander, S. P., Mathie, A., Peters, J. A., Veale, E. L., Striessnig, J., Kelly, E., Armstrong, J. F., Faccenda, E., Harding, S. D., Pawson, A. J., Southan, C., Davies, J. A., Aldrich, R. W., Attali, B., Baggetta, A. M., Becirovic, E., Biel, M., Bill, R. M., Catterall, W. A., ... Zhu, M. (2021).

THE CONCISE GUIDE TO PHARMACOLOGY 2021/22: Ion channels. *British Journal of Pharmacology*, 178(S1), S157–S245. <https://doi.org/10.1111/bph.15539>

Alexander, S. P. H., Roberts, R. E., Broughton, B. R. S., Sobey, C. G., George, C. H., Stanford, S. C., Cirino, G., Docherty, J. R., Giembycz, M. A., Hoyer, D., Insel, P. A., Izzo, A. A., Ji, Y., MacEwan, D. J., Mangum, J., Wonnacott, S., & Ahluwalia, A. (2018). Goals and practicalities of immunoblotting and immunohistochemistry: A guide for submission to the *British Journal of Pharmacology*. *British Journal of Pharmacology*, 175, 407–411. <https://doi.org/10.1111/bph.14112>

Aljunaidy, M. M., Morton, J. S., Kirschenman, R., Phillips, T., Case, C. P., Cooke, C. M., & Davidge, S. T. (2018). Maternal treatment with a placental-targeted antioxidant (MitoQ) impacts offspring cardiovascular function in a rat model of prenatal hypoxia. *Pharmacological Research*, 134, 332–342. <https://doi.org/10.1016/j.phrs.2018.05.006>

Anton, L., DeVine, A., Polyak, E., Olarerin-George, A., Brown, A. G., Falk, M. J., & Elovitz, M. A. (2019). HIF-1 α stabilization increases miR-210 eliciting first trimester extravillous trophoblast mitochondrial dysfunction. *Frontiers in Physiology*, 10, 699. <https://doi.org/10.3389/fphys.2019.00699>

Bavelloni, A., Ramazzotti, G., Poli, A., Piazzini, M., Focaccia, E., Blalock, W., & Faenza, I. (2017). miRNA-210: A current overview. *Anticancer Research*, 37, 6511–6521. <https://doi.org/10.21873/anticancer.12107>

Botting, K. J., Skeffington, K. L., Niu, Y., Allison, B. J., Brain, K. L., Itani, N., Beck, C., Logan, A., Murray, A. J., Murphy, M. P., & Giussani, D. A. (2020). Translatable mitochondria-targeted protection against programmed cardiovascular dysfunction. *Science Advances*, 6, eabb1929. <https://doi.org/10.1126/sciadv.abb1929>

Chan, S. Y., Zhang, Y. Y., Hemann, C., Mahoney, C. E., Zweier, J. L., & Loscalzo, J. (2009). MicroRNA-210 controls mitochondrial metabolism during hypoxia by repressing the iron-sulfur cluster assembly proteins ISCU1/2. *Cell Metabolism*, 10, 273–284. <https://doi.org/10.1016/j.cmet.2009.08.015>

Chan, Y. C., Banerjee, J., Choi, S. Y., & Sen, C. K. (2012). miR-210: The master hypoxamir. *Microcirculation*, 19, 215–223. <https://doi.org/10.1111/j.1549-8719.2011.00154.x>

Chaplin, N. L., Nieves-Cintrón, M., Fresquez, A. M., Navedo, M. F., & Amberg, G. C. (2015). Arterial smooth muscle mitochondria amplify hydrogen peroxide microdomains functionally coupled to L-type calcium channels. *Circulation Research*, 117, 1013–1023. <https://doi.org/10.1161/CIRCRESAHA.115.306996>

Cheranov, S. Y., & Jaggar, J. H. (2004). Mitochondrial modulation of Ca²⁺ sparks and transient K_{Ca} currents in smooth muscle cells of rat cerebral arteries. *The Journal of Physiology*, 556, 755–771. <https://doi.org/10.1113/jphysiol.2003.059568>

Chouchani, E. T., Pell, V. R., Gaude, E., Aksentijevic, D., Sundier, S. Y., Robb, E. L., Logan, A., Nadtochiy, S. M., Ord, E. N. J., Smith, A. C., Eyassu, F., Shirley, R., Hu, C. H., Dare, A. J., James, A. M., Rogatti, S., Hartley, R. C., Eaton, S., Costa, A. S. H., ... Murphy, M. P. (2014). Ischaemic accumulation of succinate controls reperfusion injury through mitochondrial ROS. *Nature*, 515, 431–435. <https://doi.org/10.1038/nature13909>

Cicchillitti, L., Di Stefano, V., Isaia, E., Crimaldi, L., Fasanaro, P., Ambrosino, V., Antonini, A., Capogrossi, M. C., Gaetano, C., Piaggio, G., & Martelli, F. (2012). Hypoxia-inducible factor 1- α induces miR-210 in normoxic differentiating myoblasts. *The Journal of Biological Chemistry*, 287, 44761–44771. <https://doi.org/10.1074/jbc.M112.421255>

Colleoni, F., Padmanabhan, N., Yung, H. W., Watson, E. D., Cetin, I., Tissot van Patot, M. C., Burton, G. J., & Murray, A. J. (2013). Suppression of mitochondrial electron transport chain function in the hypoxic human placenta: A role for miRNA-210 and protein synthesis inhibition. *PLoS ONE*, 8, e55194. <https://doi.org/10.1371/journal.pone.0055194>

- Curtis, M. J., Alexander, S., Cirino, G., Docherty, J. R., George, C. H., Giembycz, M. A., Hoyer, D., Insel, P. A., Izzo, A. A., Ji, Y., MacEwan, D. J., Sobey, C. G., Stanford, S. C., Teixeira, M. M., Wonnacott, S., & Ahluwalia, A. (2018). Experimental design and analysis and their reporting II: Updated and simplified guidance for authors and peer reviewers. *British Journal of Pharmacology*, *175*, 987–993. <https://doi.org/10.1111/bph.14153>
- Ding, J., & Wang, D. Z. (2011). "RISCing" the heart: In vivo identification of cardiac microRNA targets by RISCome. *Circulation Research*, *108*, 3–5. <https://doi.org/10.1161/CIRCRESAHA.110.238584>
- Ducsay, C. A., Goyal, R., Pearce, W. J., Wilson, S., Hu, X. Q., & Zhang, L. (2018). Gestational hypoxia and developmental plasticity. *Physiological Reviews*, *98*, 1241–1334. <https://doi.org/10.1152/physrev.00043.2017>
- Fato, R., Bergamini, C., Bortolus, M., Maniero, A. L., Leoni, S., Ohnishi, T., & Lenaz, G. (2009). Differential effects of mitochondrial complex I inhibitors on production of reactive oxygen species. *Biochimica et Biophysica Acta*, *1787*, 384–392. <https://doi.org/10.1016/j.bbabi.2008.11.003>
- Favaro, E., Ramachandran, A., McCormick, R., Gee, H., Blancher, C., Crosby, M., Devlin, C., Blick, C., Buffa, F., Li, J. L., Vojnovic, B., Pires das Neves, R., Glazer, P., Iborra, F., Ivan, M., Ragoussis, J., & Harris, A. L. (2010). MicroRNA-210 regulates mitochondrial free radical response to hypoxia and Krebs cycle in cancer cells by targeting iron sulfur cluster protein ISCU. *PLoS ONE*, *5*, e10345. <https://doi.org/10.1371/journal.pone.0010345>
- Freed, J. K., & Gutterman, D. D. (2013). Mitochondrial reactive oxygen species and vascular function: Less is more. *Arteriosclerosis, Thrombosis, and Vascular Biology*, *33*, 673–675. <https://doi.org/10.1161/ATVBAHA.13.301039>
- Ganguly, E., Kirschenman, R., Spaans, F., Holody, C. D., Phillips, T. E. J., Case, C. P., Cooke, C. M., Murphy, M. P., Lemieux, H., & Davidge, S. T. (2021). Nanoparticle-encapsulated antioxidant improves placental mitochondrial function in a sexually dimorphic manner in a rat model of prenatal hypoxia. *The FASEB Journal*, *35*, e21338. <https://doi.org/10.1096/fj.202002193R>
- Hu, X. Q., Dasgupta, C., Song, R., Romero, M., Wilson, S. M., & Zhang, L. (2021). MicroRNA-210 mediates hypoxia-induced repression of spontaneous transient outward currents in sheep uterine arteries during gestation. *Hypertension*, *77*, 1412–1427. <https://doi.org/10.1161/HYPERTENSIONAHA.120.16831>
- Hu, X. Q., Dasgupta, C., Xiao, D., Huang, X., Yang, S., & Zhang, L. (2017). MicroRNA-210 targets ten-eleven translocation methylcytosine dioxygenase 1 and suppresses pregnancy-mediated adaptation of large conductance Ca²⁺-activated K⁺ channel expression and function in ovine uterine arteries. *Hypertension*, *70*, 601–612. <https://doi.org/10.1161/HYPERTENSIONAHA.117.09864>
- Hu, X. Q., Huang, X., Xiao, D., & Zhang, L. (2016). Direct effect of chronic hypoxia in suppressing large conductance Ca²⁺-activated K⁺ channel activity in ovine uterine arteries via increasing oxidative stress. *The Journal of Physiology*, *594*, 343–356. <https://doi.org/10.1113/JP271626>
- Hu, X. Q., Song, R., Romero, M., Dasgupta, C., Huang, X., Holguin, M. A., Williams, V. S., Xiao, D., Wilson, S. M., & Zhang, L. (2019). Pregnancy increases Ca²⁺ sparks/spontaneous transient outward currents and reduces uterine arterial myogenic tone. *Hypertension*, *73*, 691–702. <https://doi.org/10.1161/HYPERTENSIONAHA.118.12484>
- Hu, X. Q., Song, R., Romero, M., Dasgupta, C., Min, J., Hatcher, D., Xiao, D., Blood, A., Wilson, S. M., & Zhang, L. (2020). Gestational hypoxia inhibits pregnancy-induced upregulation of Ca²⁺ Sparks and spontaneous transient outward currents in uterine arteries via heightened endoplasmic reticulum/oxidative stress. *Hypertension*, *76*, 930–942. <https://doi.org/10.1161/HYPERTENSIONAHA.120.15235>
- Hu, X. Q., Xiao, D., Zhu, R., Huang, X., Yang, S., Wilson, S., & Zhang, L. (2011). Pregnancy upregulates large-conductance Ca²⁺-activated K⁺ channel activity and attenuates myogenic tone in uterine arteries. *Hypertension*, *58*, 1132–1139. <https://doi.org/10.1161/HYPERTENSIONAHA.111.179952>
- Hu, X. Q., & Zhang, L. (2021a). Hypoxia and mitochondrial dysfunction in pregnancy complications. *Antioxidants (Basel)*, *10*, 405. <https://doi.org/10.3390/antiox10030405>
- Hu, X. Q., & Zhang, L. (2021b). Hypoxia and the integrated stress response promote pulmonary hypertension and preeclampsia: Implications in drug development. *Drug Discovery Today*, *26*, 2754–2773. <https://doi.org/10.1016/j.drudis.2021.07.011>
- Huang, X., Le, Q. T., & Giaccia, A. J. (2010). MiR-210—Micromanager of the hypoxia pathway. *Trends in Molecular Medicine*, *16*, 230–237. <https://doi.org/10.1016/j.molmed.2010.03.004>
- Lee, P., Chandel, N. S., & Simon, M. C. (2020). Cellular adaptation to hypoxia through hypoxia inducible factors and beyond. *Nature Reviews. Molecular Cell Biology*, *21*, 268–283. <https://doi.org/10.1038/s41580-020-0227-y>
- Lilley, E., Stanford, S. C., Kendall, D. E., Alexander, S. P., Cirino, G., Docherty, J. R., George, C. H., Insel, P. A., Izzo, A. A., Ji, Y., Panettieri, R. A., Sobey, C. G., Stefanska, B., Stephens, G., Teixeira, M., & Ahluwalia, A. (2020). ARRIVE 2.0 and the *British Journal of Pharmacology*: Updated guidance for 2020. *British Journal of Pharmacology*. <https://bpspubs.onlinelibrary.wiley.com/doi/full/10.1111/bph.15178>
- Loscalzo, J. (2010). The cellular response to hypoxia: Tuning the system with microRNAs. *The Journal of Clinical Investigation*, *120*, 3815–3817. <https://doi.org/10.1172/JCI45105>
- Ma, Q., Dasgupta, C., Li, Y., Huang, L., & Zhang, L. (2019). MicroRNA-210 downregulates ISCU and induces mitochondrial dysfunction and neuronal death in neonatal hypoxic-ischemic brain injury. *Molecular Neurobiology*, *56*, 5608–5625. <https://doi.org/10.1007/s12035-019-1491-8>
- Maio, N., Kim, K. S., Singh, A., & Rouault, T. A. (2017). A single adaptable cochaperone-scaffold complex delivers nascent iron-sulfur clusters to mammalian respiratory chain complexes I–III. *Cell Metabolism*, *25*(945–953), e946. <https://doi.org/10.1016/j.cmet.2017.03.010>
- Marin, R., Chiarello, D. I., Abad, C., Rojas, D., Toledo, F., & Sobrevia, L. (2020). Oxidative stress and mitochondrial dysfunction in early-onset and late-onset preeclampsia. *Biochimica et Biophysica Acta - Molecular Basis of Disease*, *1866*, 165961. <https://doi.org/10.1016/j.bbadis.2020.165961>
- Matheson, H., Veerbeek, J. H., Charnock-Jones, D. S., Burton, G. J., & Yung, H. W. (2016). Morphological and molecular changes in the murine placenta exposed to normobaric hypoxia throughout pregnancy. *The Journal of Physiology*, *594*, 1371–1388. <https://doi.org/10.1113/JP271073>
- Muralimanotharan, S., Maloyan, A., Mele, J., Guo, C., Myatt, L. G., & Myatt, L. (2012). MIR-210 modulates mitochondrial respiration in placenta with preeclampsia. *Placenta*, *33*, 816–823. <https://doi.org/10.1016/j.placenta.2012.07.002>
- Mutharasan, R. K., Nagpal, V., Ichikawa, Y., & Ardehali, H. (2011). microRNA-210 is upregulated in hypoxic cardiomyocytes through Akt- and p53-dependent pathways and exerts cytoprotective effects. *American Journal of Physiology. Heart and Circulatory Physiology*, *301*, H1519–H1530. <https://doi.org/10.1152/ajpheart.01080.2010>
- Nikolaienko, R., Bovo, E., & Zima, A. V. (2018). Redox dependent modifications of ryanodine receptor: Basic mechanisms and implications in heart diseases. *Frontiers in Physiology*, *9*, 1775. <https://doi.org/10.3389/fphys.2018.01775>
- Nuzzo, A. M., Camm, E. J., Sferruzzi-Perri, A. N., Ashmore, T. J., Yung, H. W., Cindrova-Davies, T., Spiroski, A. M., Sutherland, M. R., Logan, A., Austin-Williams, S., Burton, G. J., Rolfo, A., Todros, T., Murphy, M. P., & Giussani, D. A. (2018). Placental adaptation to early-onset hypoxic pregnancy and mitochondria-targeted antioxidant therapy in a rodent model. *The American Journal of Pathology*, *188*, 2704–2716. <https://doi.org/10.1016/j.ajpath.2018.07.027>
- Percie du Sert, N., Hurst, V., Ahluwalia, A., Alam, S., Avey, M. T., Baker, M., Browne, W. J., Clark, A., Cuthill, I. C., Dirnagl, U., Emerson, M.,

- Garner, P., Holgate, S. T., Howells, D. W., Karp, N. A., Lazic, S. E., Lidster, K., MacCallum, C. J., Macleod, M., ... Würbel, H. (2020). The ARRIVE guidelines 2.0: Updated guidelines for reporting animal research. *PLoS Biology*, 18(7), e3000410. <https://doi.org/10.1371/journal.pbio.3000410>
- Phillips, T. J., Scott, H., Menassa, D. A., Bignell, A. L., Sood, A., Morton, J. S., Akagi, T., Azuma, K., Rogers, M. F., Gilmore, C. E., Inman, G. J., Grant, S., Chung, Y., Aljunaidy, M. M., Cooke, C. L., Steinkraus, B. R., Pocklington, A., Logan, A., Collett, G. P., ... Case, C. P. (2017). Treating the placenta to prevent adverse effects of gestational hypoxia on fetal brain development. *Scientific Reports*, 7, 9079. <https://doi.org/10.1038/s41598-017-06300-1>
- Rossmann, M. J., Santos-Parker, J. R., Steward, C. A. C., Bispham, N. Z., Cuevas, L. M., Rosenberg, H. L., Woodward, K. A., Chonchol, M., Gioscia-Ryan, R. A., Murphy, M. P., & Seals, D. R. (2018). Chronic supplementation with a mitochondrial antioxidant (MitoQ) improves vascular function in healthy older adults. *Hypertension*, 71, 1056–1063. <https://doi.org/10.1161/HYPERTENSIONAHA.117.10787>
- Sheak, J. R., Yan, S., Weise-Cross, L., Ahmadian, R., Walker, B. R., Jernigan, N. L., & Resta, T. C. (2020). PKCbeta and reactive oxygen species mediate enhanced pulmonary vasoconstrictor reactivity following chronic hypoxia in neonatal rats. *American Journal of Physiology. Heart and Circulatory Physiology*, 318, H470–H483. <https://doi.org/10.1152/ajpheart.00629.2019>
- Soleymanlou, N., Jurisica, I., Nevo, O., Ietta, F., Zhang, X., Zamudio, S., Post, M., & Caniggia, I. (2005). Molecular evidence of placental hypoxia in preeclampsia. *The Journal of Clinical Endocrinology and Metabolism*, 90, 4299–4308. <https://doi.org/10.1210/jc.2005-0078>
- Song, R., Hu, X. Q., Romero, M., Holguin, M. A., Kagabo, W., Xiao, D., Wilson, S. M., & Zhang, L. (2021). Ryanodine receptor subtypes regulate Ca²⁺ sparks/spontaneous transient outward currents and myogenic tone of uterine arteries in pregnancy. *Cardiovascular Research*, 117, 792–804. <https://doi.org/10.1093/cvr/cvaa089>
- Tang, X. D., Daggett, H., Hanner, M., Garcia, M. L., McManus, O. B., Brot, N., Weissbach, H., Heinemann, S. H., & Hoshi, T. (2001). Oxidative regulation of large conductance calcium-activated potassium channels. *The Journal of General Physiology*, 117, 253–274. <https://doi.org/10.1085/jgp.117.3.253>
- Tang, X. D., Garcia, M. L., Heinemann, S. H., & Hoshi, T. (2004). Reactive oxygen species impair Slo1 BK channel function by altering cysteine-mediated calcium sensing. *Nature Structural & Molecular Biology*, 11, 171–178. <https://doi.org/10.1038/nsmb725>
- Tong, W., & Giussani, D. A. (2019). Preeclampsia link to gestational hypoxia. *Journal of Developmental Origins of Health and Disease*, 10, 322–333. <https://doi.org/10.1017/S204017441900014X>
- Vaka, V. R., McMaster, K. M., Cornelius, D. C., Ibrahim, T., Jayaram, A., Usry, N., Cunningham, M. W. Jr., Amaral, L. M., & LaMarca, B. (2019). Natural killer cells contribute to mitochondrial dysfunction in response to placental ischemia in reduced uterine perfusion pressure rats. *American Journal of Physiology. Regulatory, Integrative and Comparative Physiology*, 316, R441–R447. <https://doi.org/10.1152/ajpregu.00279.2018>
- Vaka, V. R., McMaster, K. M., Cunningham, M. W. Jr., Ibrahim, T., Hazlewood, R., Usry, N., Cornelius, D. C., Amaral, L. M., & LaMarca, B. (2018). Role of mitochondrial dysfunction and reactive oxygen species in mediating hypertension in the reduced uterine perfusion pressure rat model of preeclampsia. *Hypertension*, 72, 703–711. <https://doi.org/10.1161/HYPERTENSIONAHA.118.11290>
- Vangrieken, P., Al-Nasiry, S., Bast, A., Leermakers, P. A., Tulen, C. B. M., Janssen, G. M. J., Kaminski, I., Geomini, I., Lemmens, T., Schiffers, P. M. H., van Schooten, F. J., & Remels, A. H. V. (2021a). Hypoxia-induced mitochondrial abnormalities in cells of the placenta. *PLoS ONE*, 16, e0245155. <https://doi.org/10.1371/journal.pone.0245155>
- Vangrieken, P., Al-Nasiry, S., Bast, A., Leermakers, P. A., Tulen, C. B. M., Schiffers, P. M. H., van Schooten, F. J., & Remels, A. H. V. (2021b). Placental mitochondrial abnormalities in preeclampsia. *Reproductive Sciences*, 28, 2186–2199. <https://doi.org/10.1007/s43032-021-00464-y>
- Wang, Y., & Walsh, S. W. (1998). Placental mitochondria as a source of oxidative stress in pre-eclampsia. *Placenta*, 19, 581–586. [https://doi.org/10.1016/s0143-4004\(98\)90018-2](https://doi.org/10.1016/s0143-4004(98)90018-2)
- Waypa, G. B., Marks, J. D., Guzy, R., Mungai, P. T., Schriewer, J., Dokic, D., & Schumacker, P. T. (2010). Hypoxia triggers subcellular compartmental redox signaling in vascular smooth muscle cells. *Circulation Research*, 106, 526–535. <https://doi.org/10.1161/CIRCRESAHA.109.206334>
- White, K., Lu, Y., Annis, S., Hale, A. E., Chau, B. N., Dahlman, J. E., Hemann, C., Opatowsky, A. R., Vargas, S. O., Rosas, I., Perrella, M. A., Osorio, J. C., Haley, K. J., Graham, B. B., Kumar, R., Saggari, R., Saggari, R., Wallace, W. D., Ross, D. J., ... Chan, S. Y. (2015). Genetic and hypoxic alterations of the microRNA-210-ISCU1/2 axis promote iron-sulfur deficiency and pulmonary hypertension. *EMBO Molecular Medicine*, 7, 695–713. <https://doi.org/10.15252/emmm.201404511>
- Wu, L., Zhou, H., Lin, H., Qi, J., Zhu, C., Gao, Z., & Wang, H. (2012). Circulating microRNAs are elevated in plasma from severe preeclamptic pregnancies. *Reproduction*, 143, 389–397. <https://doi.org/10.1530/REP-11-0304>
- Xiao, D., Hu, X. Q., Huang, X., Zhou, J., Wilson, S. M., Yang, S., & Zhang, L. (2013). Chronic hypoxia during gestation enhances uterine arterial myogenic tone via heightened oxidative stress. *PLoS ONE*, 8, e73731. <https://doi.org/10.1371/journal.pone.0073731>
- Yan, Y., Liu, J., Wei, C., Li, K., Xie, W., Wang, Y., & Cheng, H. (2008). Bidirectional regulation of Ca²⁺ sparks by mitochondria-derived reactive oxygen species in cardiac myocytes. *Cardiovascular Research*, 77, 432–441. <https://doi.org/10.1093/cvr/cvm047>
- Zamudio, S., Postigo, L., Illsley, N. P., Rodriguez, C., Heredia, G., Brimacombe, M., Echalar, L., Torricos, T., Tellez, W., Maldonado, I., Balanza, E., Alvarez, T., Ameller, J., & Vargas, E. (2007). Maternal oxygen delivery is not related to altitude- and ancestry-associated differences in human fetal growth. *The Journal of Physiology*, 582, 883–895. <https://doi.org/10.1113/jphysiol.2007.130708>
- Zhang, Y., Fei, M., Xue, G., Zhou, Q., Jia, Y., Li, L., Xin, H., & Sun, S. (2012). Elevated levels of hypoxia-inducible microRNA-210 in pre-eclampsia: New insights into molecular mechanisms for the disease. *Journal of Cellular and Molecular Medicine*, 16, 249–259. <https://doi.org/10.1111/j.1582-4934.2011.01291.x>
- Zinovkin, R. A., & Zamyatnin, A. A. (2019). Mitochondria-targeted drugs. *Curr. Molecular Pharmacology*, 12, 202–214. <https://doi.org/10.2174/1874467212666181127151059>
- Zissimopoulos, S., & Lai, F. A. (2006). Redox regulation of the ryanodine receptor/calcium release channel. *Biochemical Society Transactions*, 34, 919–921. <https://doi.org/10.1042/BST0340919>

SUPPORTING INFORMATION

Additional supporting information can be found online in the Supporting Information section at the end of this article.

How to cite this article: Hu, X.-Q., Song, R., Dasgupta, C., Romero, M., Juarez, R., Hanson, J., Blood, A. B., Wilson, S. M., & Zhang, L. (2022). MicroRNA-210-mediated mtROS confer hypoxia-induced suppression of STOCs in ovine uterine arteries. *British Journal of Pharmacology*, 179(19), 4640–4654. <https://doi.org/10.1111/bph.15914>